

## 硅胶的表面硫醇化改性及对水溶液中罗丹明 B 的固载

杨汉培<sup>\*,1,2</sup> 俞咪虹<sup>1</sup> 傅小飞<sup>1</sup> 吴俊明<sup>1,2</sup>

(<sup>1</sup> 河海大学浅水湖泊综合治理与资源开发教育部重点实验室, 河海大学环境学院, 南京 210098)

(<sup>2</sup> 河海大学淮安研究院, 淮安 223001)

**摘要:** 运用  $\gamma$ -巯丙基三乙氧基硅烷对硅胶表面硫醇化修饰改性, 红外及拉曼光谱分析表明硅胶的表面硫醇化借助硅胶表面羟基与  $\gamma$ -巯丙基二乙氧基硅烷间的化学键联实现。实验条件下改性硅胶对水体罗丹明 B 的吸附性能明显提升, 改性硅胶表面罗丹明 B 的吸附动力学符合准二级动力学模型, 吸附等温线服从 Langmuir 等温线规律, 由等温吸附计算得到的热力学函数变化表明吸附系自发、放热过程。吸附动力学、热力学及光谱表征均表明改性硅胶上罗丹明 B 的吸附主要为其在改性硅胶表面借助电价和共价键联的化学吸附。

**关键词:** 罗丹明 B; 硅胶; 硫醇化; 吸附; 机制

中图分类号: O613.71

文献标识码: A

文章编号: 1001-4861(2015)03-0571-09

DOI: 10.11862/CJIC.2015.064

## Thiolated Silica Gel: Synthesis and Immobilization of Rhodamine B from Aqueous Solution

YANG Han-Pei<sup>\*,1,2</sup> YU Mi-Hong<sup>1</sup> FU Xiao-Fei<sup>1</sup> WU Jun-Ming<sup>1,2</sup>

(<sup>1</sup>Key Laboratory of Integrated Regulation and Resource Development on Shallow Lakes,  
Ministry of Education, College of Environment, Hohai University, Nanjing 210098, China)

(<sup>2</sup>Huaian Research Institute, Hohai University, Huaian, Jiangsu 223002, China)

**Abstract:** A thiolated silica gel was obtained by treating the as-prepared pristine silica gel with  $\gamma$ -mercaptopropyltriethoxysilane through an impregnation route. The FTIR and Raman spectroscopy results indicate that the thiolation of silica gel is achieved by attaching  $\gamma$ -mercaptopropyltriethoxysilane onto the surface of silica gel via a chemical linking. The results for batch removal of Rhodamine B(RhB) from aqueous solution by the thiolated silica gel demonstrate that the thiolated silica gel can effectively adsorb RhB under a wide range of conditions. The data of adsorption kinetics are fitted well with the pseudo-second-order model, and the equilibrium data are well described by the typical Langmuir adsorption isotherm. The thermodynamic derivation shows an exothermic and spontaneous nature of adsorption process with a high value of enthalpy change. The adsorption kinetics, isotherm and thermodynamics suggest a mechanism involving chemisorptions of RhB on thiolated silica gel as confirmed by FTIR and Raman spectroscopy.

**Key words:** Rhodamine B; silica gel; thiolation; adsorption; mechanism

At present, more than 100 000 types of dyes are used in plastics, paper and pulp, cosmetics, leather,

textiles and food industries<sup>[1-2]</sup>. Dyes can be noticed at concentration even as low as  $1 \text{ mg} \cdot \text{L}^{-1}$ , which makes

收稿日期: 2014-10-04。收修稿日期: 2014-12-09。

河海大学淮安研究院开放基金(No.1061-51402012), 江苏省高校优势学科建设工程资助项目。

\*通讯联系人。E-mail: yanghanpei@hhu.edu.cn

it unfit for human consumption<sup>[3]</sup>. The complex aromatic molecular structures owned by some dyes make them toxic or carcinogenic and also limit their biodegradation<sup>[4-5]</sup>.

Many techniques and methods for removing dyes from water have been developed, including advanced oxidation<sup>[6]</sup>, photocatalytic oxidation<sup>[7]</sup>, coagulation and flocculation<sup>[8]</sup>, membrane separation<sup>[9]</sup>. From the economic and efficiency point of view, adsorption is regarded as the most promising and widely used method to treat dye polluted effluents. Adsorption of dyes on a wide variety of materials has been comprehensively summarized<sup>[10]</sup>. Silica gel has a large surface area, mechanical stability, chemical inert and is easily to be modified<sup>[11]</sup>. Silicious materials have been widely applied to treat heavy metals in water<sup>[12-16]</sup>. At present, their application to adsorption of dyes molecules has aroused more and more attentions<sup>[17-19]</sup>. Monash et al.<sup>[20]</sup> synthesized a sulfated mesoporous MCM-41 with a large surface area as a promising adsorbent to treat polluted water containing dyestuff. Arabinda et al.<sup>[21]</sup> synthesized hollow silica nanoparticles using anionic surfactant templating method, and the fluorescence spectroscopy results show that the hollow nanoparticles entrap the dye in trace amounts effectively. However, among the most of studies, the adsorption mechanisms are less involved<sup>[20]</sup>.

In this study, a thiolated silica gel treated by coupling of as-prepared pristine silica gel with  $\gamma$ -mercaptopropyltriethoxysilane was synthesized, and the surface nature of modified silica gel was investigated. The removal of aqueous Rhodamine B (RhB) by the adsorption of the modified silica gel and the effects of factors such as pH, initial concentration of RhB, adsorbent dosage, and adsorption temperature were evaluated. The adsorption kinetics, isotherms, thermodynamics were studied and the adsorption mechanism was proposed and discussed.

## 1 Experimental

### 1.1 Materials and methods

The tetraethylorthosilicate (TEOS, Tetraethoxysilane CAS No.562-90-3) of analytical grade (AR)

used as the precursor of pristine silica gel was purchased from Sinopharm Chemical Reagent Co., Ltd.  $\gamma$ -Mercaptopropyltriethoxysilane (MPTS, AR) was supplied by Capatue Chemical Co., Ltd. (Nanjing, China). The dye RhB was received from Sinopharm Chemical Reagent Co., Ltd. The other chemicals used were all of commercial analytical grade, and were used without further purification. Deionized water was used throughout.

The pH value of the solution was determined with a PB-10 pH meter (Sartorius, Germany). Concentration of RhB was analyzed on a V-5100 visible spectrophotometer (Yuanxi, China). SEM images were obtained by a field emission S-4800 SEM (Hitachi, Japan). Infrared spectra of KBr powder-pressed pellets were recorded on a Tensor 37 spectrometer (Bruker, Germany). Raman spectra were obtained on an Invia laser Raman spectrophotometer (Renishaw, England) with a laser resource used for excitation at wavelength of 633 nm. The nitrogen adsorption/desorption isotherms were measured at 77 K with an automatic physisorption analyzer ASAP 2020 (Micromeritics, USA). The surface area was determined by the Brunauer-Emmett-Teller (BET) method and the pore size was obtained by the Barrett-Joyner-Halenda (BJH) calculation. The surface zeta potentials of the adsorbents were measured using a Zetasizer (Malvern, England).

### 1.2 Preparation of pristine silica gel

Pristine silica gel ( $\text{pSiO}_2$ ) was prepared through a sol-gel route according to Pitoniak et al.<sup>[22]</sup>. In a typical synthesis, 10 mL deionized water, 20 mL ethanol and 10 mL TEOS were mixed under vigorous stirring. After further stirring for 10 min, nitric acid ( $1 \text{ mol} \cdot \text{L}^{-1}$ , 2 mL) and hydrofluoric acid (3wt%, 2 mL), which were used as catalysts to increase the hydrolysis rate of TEOS and to reduce the gelation time, were added to this mixture solution dropwise under magnetic stirring. The obtained sol was covered and aged at room temperature for 24 h and dried in an oven at 60 °C overnight, the resultant gel was washed with deionized water repeatedly until the supernatant was neutral, it was then ground and dried

in an oven at 100 °C for 24 h, the obtained material was finally calcined at 550 °C in a muffle furnace for 4 h.

### 1.3 Preparation of modified silica gel

Modified silica gel(mSiO<sub>2</sub>) was prepared by an impregnation method as follows: 25 g pSiO<sub>2</sub> was mixed with 250 mL *N,N*-dimethylformamide (DMF) solution containing 25 mL MPTS into a three-necked flask. The mixture was stirred and heated in reflux for 5 h under nitrogen atmosphere. The resultant particles were washed with ethanol several times to remove the solvent or unconverted MPTS. The collected particles were dried in an oven at 60 °C for 4 h.

### 1.4 Adsorption tests

Desired amounts of pSiO<sub>2</sub> or mSiO<sub>2</sub> were introduced into conical flasks with plug, to which 50 mL of RhB solution with various concentrations at adjusted pH value was added. The solutions were agitated in an orbital shaker at a constant speed of 150 r·min<sup>-1</sup> at different temperatures (25, 35 and 45 °C). The two phases were separated by centrifugation at 4 000 r·min<sup>-1</sup>. The final RhB concentration in solution was analyzed on visible spectrophotometer by monitoring their absorbance at the optimal wavelength of 554 nm. The equilibrium RhB adsorption capacity ( $q_e$ ) and removal rate (R) were calculated for each sample by using the expression reported<sup>[6]</sup>. All experiments were conducted by batch technique and the experimental data were the average of duplicate determinations.

### 1.5 Modeling of adsorption data and thermodynamics calculation

The adsorption kinetic data of RhB measured on pSiO<sub>2</sub> and mSiO<sub>2</sub>, respectively, were analyzed in terms of pseudo-first-order and pseudo-second-order adsorption equations. The two most common isotherms, Freundlich and Langmuir models were employed for modeling equilibrium adsorption of RhB obtained on pSiO<sub>2</sub> or mSiO<sub>2</sub>. The changes in Gibbs free energies were calculated based on the equation reported<sup>[23]</sup>, the changes in enthalpies and entropies of adsorption process were obtained from each intercept and slope of linear form of Van't Hoff equations.

## 2 Results and discussion

### 2.1 FTIR and Raman spectroscopy

Fig.1 presents the IR spectra acquired on pSiO<sub>2</sub> and mSiO<sub>2</sub>. The bands at wave number around 3 425 cm<sup>-1</sup> and 1 630 cm<sup>-1</sup> correspond to the stretching and bending vibrations of -OH (preferentially from the adsorption of H<sub>2</sub>O), respectively, the peaks of -OH in aggregative silanol groups (Si-OH) are overlapped with the peak from H<sub>2</sub>O<sup>[24]</sup>. The broad peak at about 1 105 cm<sup>-1</sup> corresponds to the asymmetric stretching vibration while the peaks around 805 and 470 cm<sup>-1</sup> are attributed to the symmetric and deformation stretching vibration of Si-O-Si, respectively<sup>[16]</sup>. The band centered at 970 cm<sup>-1</sup> represents the stretching vibration of Si-O in silanol groups<sup>[14]</sup>.

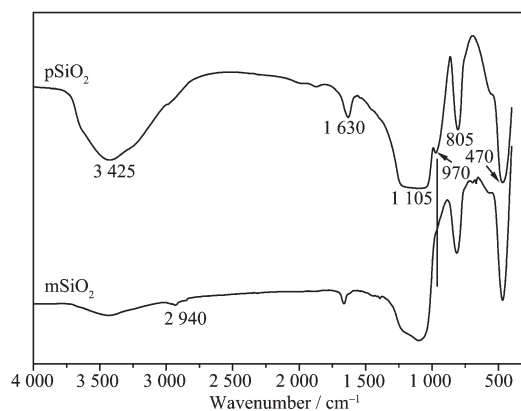
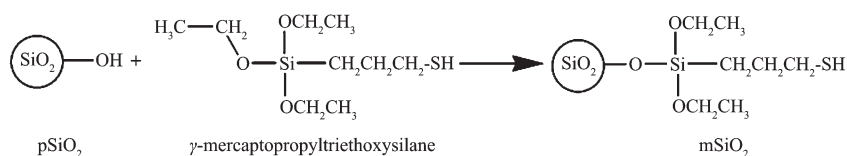


Fig.1 FTIR spectra for pSiO<sub>2</sub> and mSiO<sub>2</sub>

Compared to the spectrum on pSiO<sub>2</sub>, the peak at around 970 cm<sup>-1</sup>, which represents the Si-O in silanol groups, is not observed on the spectrum of mSiO<sub>2</sub>, accompanying a significant decreasing in intensity of peaks from -OH, this may be an evidence for the reaction between silanol groups and coupling molecules, and may imply a mechanism in scheme 1.

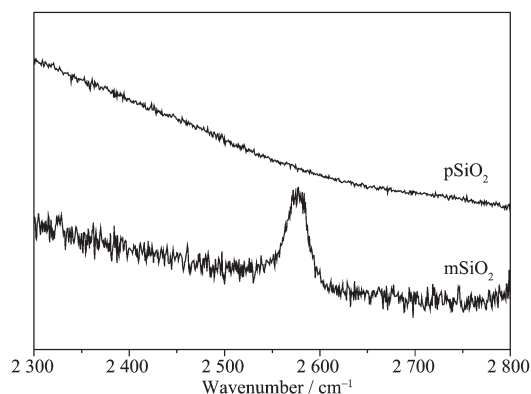
The spectrum on mSiO<sub>2</sub> shows a new weak band at 2 935 cm<sup>-1</sup> which represents the asymmetric stretching vibration from -CH in -CH<sub>2</sub> or -CH<sub>3</sub> groups. However, it is different from the results reported<sup>[25]</sup>, the absorption peak corresponds to mercapto groups is neither observed on mSiO<sub>2</sub>, probably because of the limited sensitivity of the instrument under our measuring conditions.

The mercapto groups show a strong intensity on



Scheme 1 Possible route for silica gel modification

Raman spectra at the wave number of 2 600~2 500  $\text{cm}^{-1}$  [26]. As shown in Fig.2, an evident peak appears at around 2 580  $\text{cm}^{-1}$  on the spectrum of mSiO<sub>2</sub>, confirming the modification process in Scheme 1.

Fig.2 Raman spectra acquired on pSiO<sub>2</sub> and mSiO<sub>2</sub>

## 2.2 Surface analysis

Fig.3 shows the SEM images of pSiO<sub>2</sub> and mSiO<sub>2</sub>. The surface feature of modified silica gel and that of the pristine are different, a rough and heterogeneous surface is observed on pSiO<sub>2</sub>, while a uniform aggregation of sphere-type particles are obtained on

mSiO<sub>2</sub> as shown in Fig.3(b).

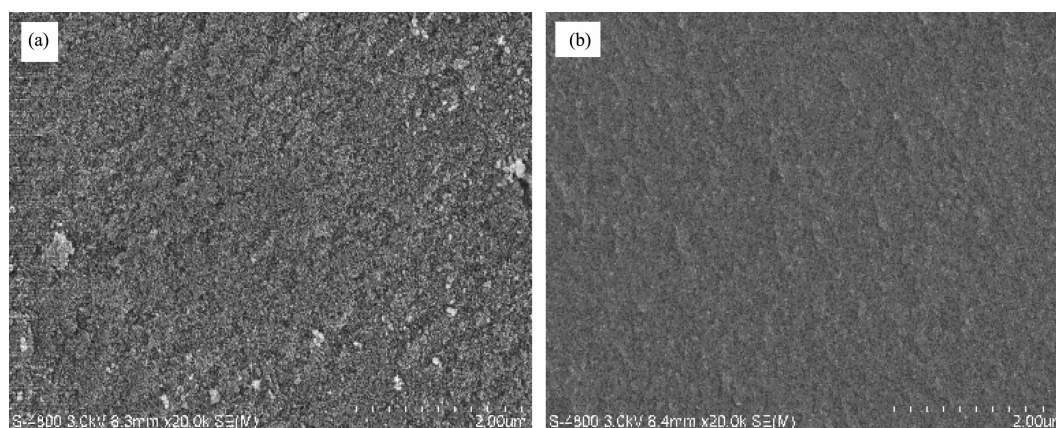
As listed in Table 1, the mSiO<sub>2</sub> shows an overall decrease in total pore volume, specific surface area and the average pore diameter compared to that of pSiO<sub>2</sub>, which could be attributed to the chemical grafting of MPTS molecules on the mSiO<sub>2</sub> that partially precludes the adsorbing of nitrogen molecules [27]. The modification process mainly changes the surface properties of the material rather than enlarging the surface area or changing the pore properties.

$\zeta$  potential for pSiO<sub>2</sub> and mSiO<sub>2</sub> is shown in Fig. 4. The pH value at zero point for charge ( $\text{pH}_{\text{ZPC}}$ ) of pSiO<sub>2</sub> is about 2.3, which is in accord with literature report [28]. The  $\text{pH}_{\text{ZPC}}$  of mSiO<sub>2</sub> shifts to a lower position at approximately 1.5 because of the chemical linking of acidic mercapto molecules.

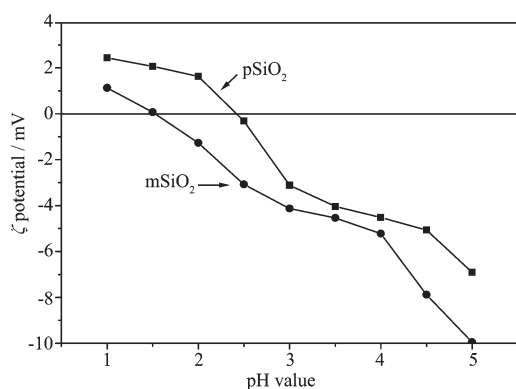
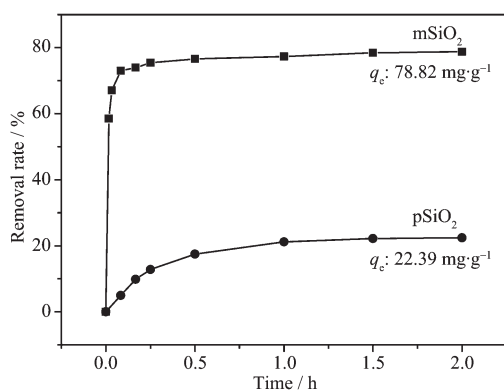
## 2.3 Adsorption of RhB towards the as-prepared adsorbents

### 2.3.1 Effect of contact time

Fig.5 presents the plots of removal percentage versus contact time of RhB on pSiO<sub>2</sub> and mSiO<sub>2</sub>,

Fig.3 SEM images of pSiO<sub>2</sub> (a) and mSiO<sub>2</sub> (b)Table 1 Surface characteristics from the N<sub>2</sub> adsorption/desorption measurement

Sample	Total pore volume / ( $\text{cm}^3 \cdot \text{g}^{-1}$ )	Specific surface area / ( $\text{m}^2 \cdot \text{g}^{-1}$ )	Average pore diameter / nm
pSiO <sub>2</sub>	1.21	379	12.81
mSiO <sub>2</sub>	0.88	305	11.5

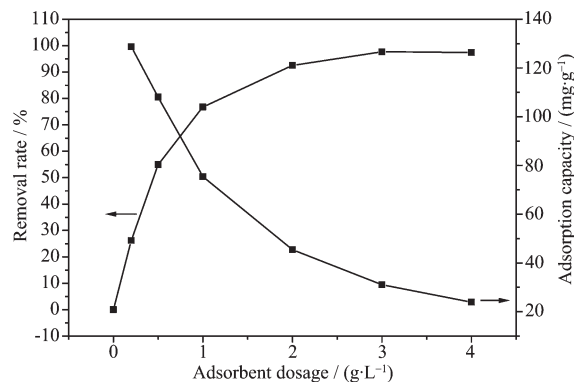
Fig.4  $\zeta$  potential on pSiO<sub>2</sub> and mSiO<sub>2</sub>Fig.5 Removal of RhB from solution onto pSiO<sub>2</sub> and mSiO<sub>2</sub> as a function of contact time at 100 mg·L<sup>-1</sup> initial concentration of RhB, 1 g·L<sup>-1</sup> adsorbents dosage, pH=6 and T=25 °C

respectively, under the same batch adsorption conditions. The adsorption property of mSiO<sub>2</sub> is significantly improved as evidenced from the comparison between the two curves in Fig.5, and the mSiO<sub>2</sub> reaches the equilibrium stage within the first 5 minutes, which is very important for dye removal in practical applications. The mSiO<sub>2</sub> saturated by RhB can be quickly reproduced by stirring it in alcohol solution (5 mol·L<sup>-1</sup>), followed by washing it with 1 mol·L<sup>-1</sup> HCl and deionized water repeatedly, the reproduced mSiO<sub>2</sub> maintains 90% of adsorption capacity on fresh mSiO<sub>2</sub> after 10 consecutive cycles.

### 2.3.2 Effect of mSiO<sub>2</sub> dosage

Fig.6 shows the adsorption of RhB as a function of mSiO<sub>2</sub> dosage. It is observed that with the raise of adsorbent dosage, the adsorption capacity decreases while the removal rate increases. The increase in the removal rate of RhB is mainly caused by the increase in

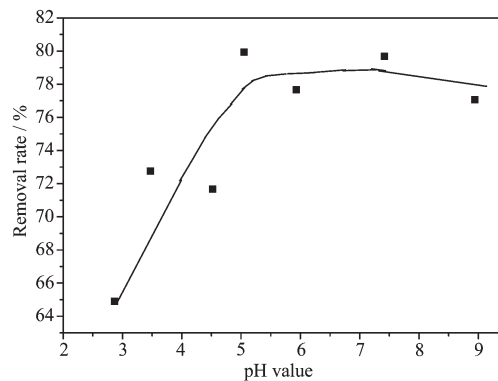
free active sites of mSiO<sub>2</sub> with the raise of mSiO<sub>2</sub> dosage. The decrease in the adsorption capacity of RhB on mSiO<sub>2</sub> is probably resulted from the aggregation of mSiO<sub>2</sub> under its higher dosage. In this study, we choose 1 g·L<sup>-1</sup> as the adsorbent dosage for high removal rate and acceptable adsorption capacity it gives.

Fig.6 Removal of aqueous RhB as a function of mSiO<sub>2</sub> dosage at 100 mg·L<sup>-1</sup> initial concentration of RhB, pH= 6, T=25 °C and contact time=1h

### 2.3.3 Effect of pH value

Fig.7 shows the adsorption of RhB as a function of pH value on the modified silica gel. With the increase in pH value, the removal percentage of RhB increases significantly between pH values of 3~6 and faintly at pH value of 6~7, the removal rate decreases when pH value exceeds 7.

The dependence of removal quantity on pH value of the RhB solution correlates mainly to the charge state of mSiO<sub>2</sub> particles and RhB molecules. The mSiO<sub>2</sub> is totally negatively charged within our pH

Fig.7 Removal of aqueous RhB as a function of pH values on mSiO<sub>2</sub> at 100 mg·L<sup>-1</sup> initial RhB concentration, 1 g·L<sup>-1</sup> mSiO<sub>2</sub> content, T=25 °C and contact time=1 h

value for the pHzpc of  $\text{mSiO}_2$  as shown in Fig.4, favoring the adsorption of cationic RhB. The negative-charge density on the surface of  $\text{mSiO}_2$  increases with the increase of pH value, thereby increasing the adsorption quantity of RhB. On the other hand, RhB is an amphoteric dye with the coexistence of amine and carboxyl groups, and the  $\text{pK}_a$  of  $-\text{COOH}$  in RhB is about 4.0<sup>[28]</sup>, it will dissociate and reduce the its positive-charge density with pH value above 4, thus making it get on the state of adverse adsorption. If the electrostatic attraction is the main interaction between  $\text{mSiO}_2$  and RhB, the maximum removal capacity should be near the pH value of 4. But this is not the case as illustrated in Fig.7, suggesting that other interactions between  $\text{mSiO}_2$  and RhB through hydrogen<sup>[24]</sup> or covalent bonding<sup>[28-29]</sup> must be involved.

#### 2.3.4 Effect of RhB initial concentration

Adsorption results of RhB on  $\text{mSiO}_2$  as a function of RhB initial concentration are shown in Fig.8. Expected decrease is observed for removal percentage of RhB along with the increase of initial RhB

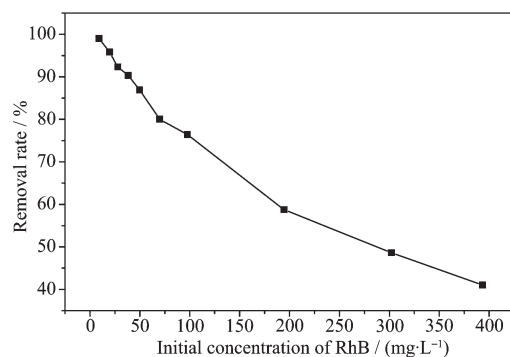


Fig.8 Removal of RhB as a function of RhB initial concentrations at  $1\text{g}\cdot\text{L}^{-1}$   $\text{mSiO}_2$  content,  $\text{pH}=6$ ,  $T=25\text{ }^\circ\text{C}$ , contact time=1 h

concentration. The available sites on the surfaces of  $\text{mSiO}_2$  are constant, the competition among the RhB ions increases with RhB concentration, and the competition results in the decrease of removal percentage because of the the electronic repulsion. However, more than 50% of RhB are absorbed even the concentration of RhB reaches  $300\text{ mg}\cdot\text{L}^{-1}$ .

#### 2.4 Adsorption kinetics

The kinetic adsorption data of RhB on  $\text{mSiO}_2$

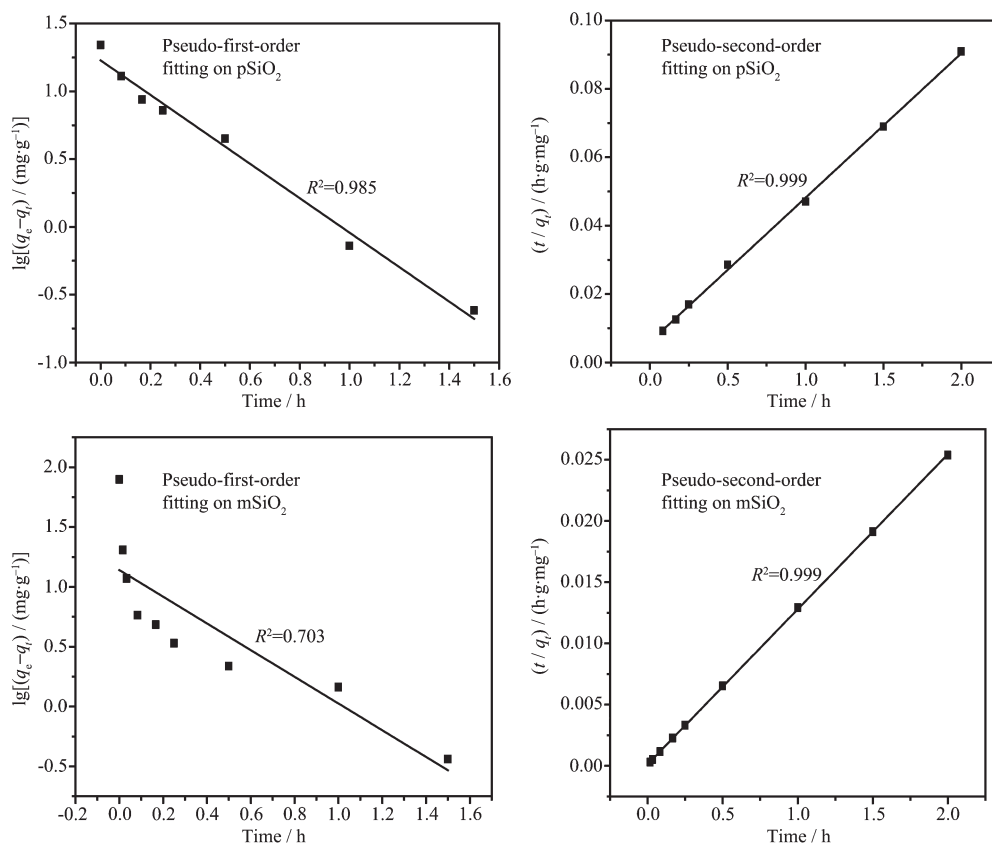


Fig.9 Adsorption kinetics of RhB on  $\text{pSiO}_2$  and  $\text{mSiO}_2$

(shown in Fig.5) are simulated with two simplified models: pseudo-first-order and pseudo-second-order models, the results are shown in Fig.9.

Both the pseudo-first and second-order model fit the experimental data well with high coefficient of determination ( $R^2$ ) for adsorption on pSiO<sub>2</sub>, however, the pseudo-first-order model fits better with an adsorption capacity calculated (21.17 mg·g<sup>-1</sup>) and matches closer to the experimental data (22.39 mg·g<sup>-1</sup>) than that from the pseudo-second-order model (25.56 mg·g<sup>-1</sup>). For the adsorption of RhB on mSiO<sub>2</sub>, the pseudo-second-order model adequately describes the kinetics of sorption of RhB with high  $R^2$ , and the calculated  $q_e$  is in good agreement with the experimental one (78.99 and 78.82 mg·g<sup>-1</sup>, respectively), indicating that chemisorptions may involve in adsorption of RhB on mSiO<sub>2</sub><sup>[30]</sup>.

## 2.5 Adsorption isotherms

In order to further determine the mechanism of RhB adsorption and evaluate the effect of temperature on the adsorption capacity, the experimental data (shown in Fig.10) are fitted to Langmuir<sup>[31]</sup> and Freundlich<sup>[32]</sup> liner equations, the results are plotted in Fig.11. As shown in Fig.10, a distinct diminution of

adsorption capacity is observed with the increase of temperature. The obtained results shown in Fig.11 indicate that the adsorption isotherm of RhB on mSiO<sub>2</sub> is better predicted by Langmuir isotherm.

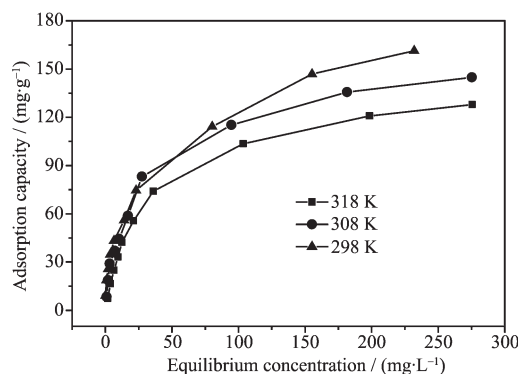


Fig.10 Adsorption isotherm of RhB on mSiO<sub>2</sub>

The Langmuir adsorption model assumes that the adsorbed layer is one molecule thick and the sites are homogeneous. As shown in Fig.11, the Langmuir isotherm has a higher  $R^2$  for the adsorption of RhB, suggesting that the adsorption process is dominated by a monolayer formation rather than a multilayer, and more importantly, implying a predominant status of the chemical adsorption<sup>[33]</sup>. The maximum adsorption capacity of RhB on mSiO<sub>2</sub> reaches 166 mg·g<sup>-1</sup>.

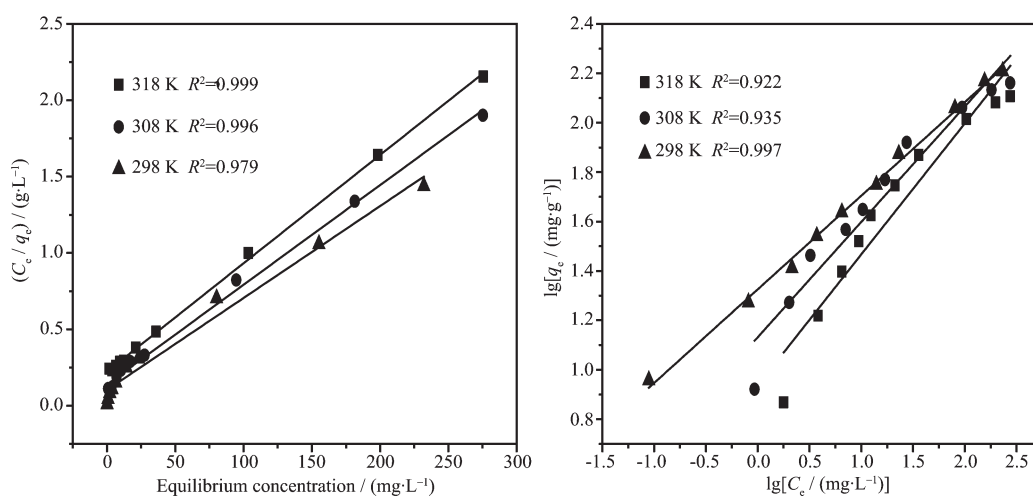


Fig.11 Langmuir (left) and Freundlich (right) isotherms fitted from the experimental data

## 2.6 Adsorption thermodynamics

The thermodynamic parameters of the adsorption process are obtained from adsorption results at various temperatures (298, 308 and 318 K). Plot of  $\ln b$  versus  $1/T$  is shown in Fig.12. The negative of values of all

$\Delta G^\ominus$  (-8.25, -7.87 and -7.19 kJ·mol<sup>-1</sup> at 298, 308 and 318 K, respectively) indicate that the adsorption process has a feasible and spontaneous nature, and the absolute value of  $\Delta G^\ominus$  decreases with the increase in temperature, suggesting that the spontaneous nature

of adsorption is inversely proportional to temperature. The negative value of  $\Delta S^\ominus$  ( $-52.0 \text{ J} \cdot \text{mol}^{-1} \cdot \text{K}^{-1}$ ) indicates the randomness decreasing during the adsorption of

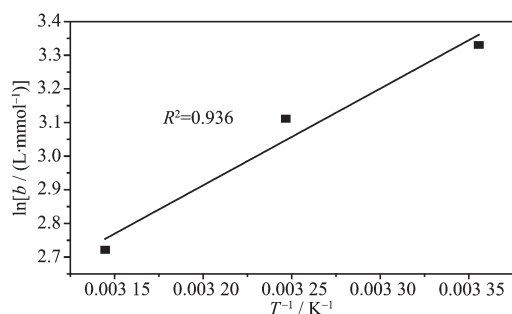


Fig.12  $\ln b$  versus  $T^{-1}$  plot for RhB adsorption on  $\text{mSiO}_2$

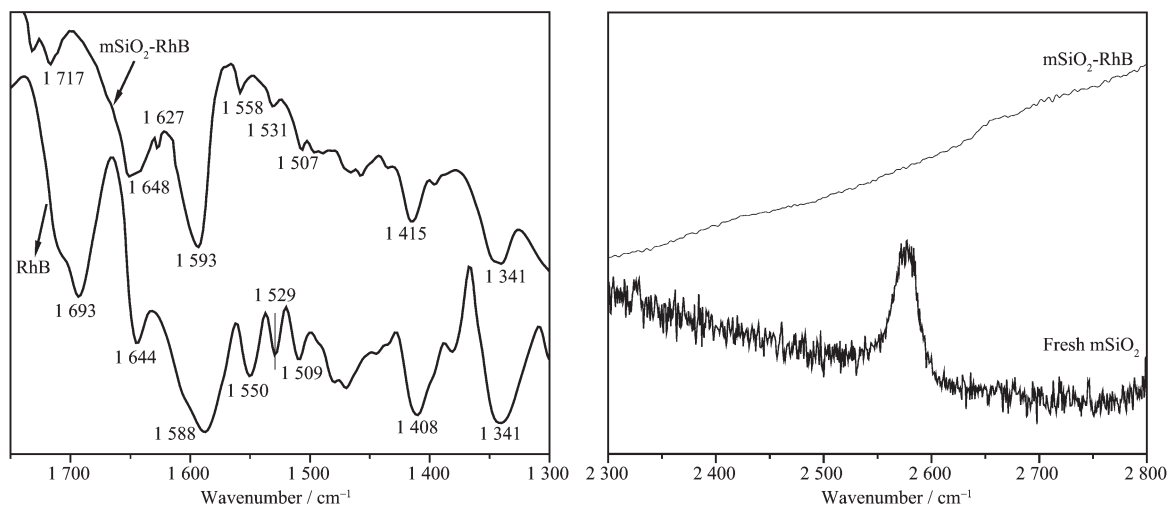


Fig.13 FTIR and Raman spectra: FTIR spectra for pure and immobilized RhB (left); Raman spectra for fresh and RhB adsorbed  $\text{mSiO}_2$  (right)

The following principal bands in the FTIR spectra of pure RhB are assigned according to literature<sup>[35]</sup>: the peak at about  $1693 \text{ cm}^{-1}$  is assigned to the stretching vibration of the carboxylic group, the peak around  $1644 \text{ cm}^{-1}$  is due to the C-N bond, peaks in the region of  $1450\sim 1600 \text{ cm}^{-1}$  are from the heterocycle and aromatic ring vibrations, and absorbance at around  $1341 \text{ cm}^{-1}$  is attributed to the C-aryl bond vibrations.

Differences are observed in the FTIR on immobilized RhB ( $\text{RhB-mSiO}_2$ ). The peak assigns to stretching vibration of carboxylic group which is shifted to a higher frequency centered at  $1717 \text{ cm}^{-1}$ , suggesting that RhB are bonded to the surface of  $\text{mSiO}_2$  through ester-like linkage. The peak from C-N vibration is overlapped in that of silanol Si-OH

RhB molecules onto  $\text{mSiO}_2$ . The negative value of  $\Delta H^\ominus$  ( $-23.9 \text{ kJ} \cdot \text{mol}^{-1}$ ) indicates the exothermic nature of adsorption and the numeric size reflects the adsorption process is probably controlled chemically<sup>[34]</sup>.

## 2.7 Adsorption mechanism

In the preceding discussion, a chemical adsorption mechanism involved in the adsorption process between RhB and  $\text{mSiO}_2$  are proposed. To verify this assumption, the FTIR and Raman spectroscopy analysis are performed and the results are displayed in Fig.13.

(bending vibration) locates near  $1648 \text{ cm}^{-1}$ . A new peak appears around  $1627 \text{ cm}^{-1}$ , this might be due to the vibration of C-N in a structure which is established through the electrostatic interaction between RhB and  $\text{mSiO}_2$ <sup>[35]</sup>.

The ester-like linkage between mercapto groups on the surface of  $\text{mSiO}_2$  and carboxylic groups in RhB during the adsorption process are further verified by Raman spectra acquired on fresh and RhB loaded  $\text{mSiO}_2$  ( $\text{mSiO}_2\text{-RhB}$ ). The band of mercapto group locates in  $2578 \text{ cm}^{-1}$  vanishes from the spectrum on  $\text{mSiO}_2\text{-RhB}$ , suggesting an adsorption mechanism through the covalent linking by esterification between -SH and -COOH. The two probably interactions between RhB and  $\text{mSiO}_2$  are illustrated in the following schematic diagram.

### 3 Conclusions

This study has shown a successful modification of pristine silica gel achieved by grafting mercapto groups onto silica gel through a covalent linking. The modified silica gel can be a good candidate for remediation of dyes in industrial effluent due to its high adsorption capacity. The adsorption capacity of modified SiO<sub>2</sub> is superior to pristine one due to the attaching of -SH groups on modified SiO<sub>2</sub>. The adsorption process is dependent on factors such as solution pH value, contact time, initial RhB concentration, adsorbents dosage and temperature. The adsorption kinetics, equilibrium and thermodynamics studies suggest that the chemisorptions dominate the uptaking of RhB by thiolated silica gel, and the FTIR and Raman spectroscopy analyses indicates that both electrovalent and covalent interaction are involved in the adsorption mechanisms.

### References:

- [1] SONG Xiao-Cui(宋晓翠), GU JING-Hua(谷景华), YAO Hong-Ying(姚红英), et al. *Chinese J. Inorg. Chem.*(无机化学学报), **2012**,**28**(6):1239-1244
- [2] Ahmed S A, Soliman E M. *Appl. Surf. Sci.*, **2013**,**284**:23-32
- [3] Malik R, Ramteke D S, Wate S R. *Waste Manage.*, **2007**,**27**(9):1129-1138
- [4] WANG Qiao-Qiao(王巧巧), NI Zhe-Ming(倪哲明), ZHANG Feng(张峰), et al. *Chinese J. Inorg. Chem.*(无机化学学报), **2009**,**25**(12):2156-2162
- [5] Barrag n B E, Costa C, M rquez M C. *Dyes Pigm.*, **2007**,**75**(1):73-81
- [6] Nawi M A, Sheilatina S S. *J. Colloid Interface Sci.*, **2012**, **372**(1):80-87
- [7] De Mendonca V R, Lopes O F, Fregonesi R P, et al. *Appl. Surf. Sci.*, **2014**,**298**:182-191
- [8] Yang Z, Yang H, Jiang Z W, et al. *J. Hazard Mater.*, **2013**, **254-255**:36-45
- [9] Zheng Y P, Yao G H, Cheng Q B, et al. *Desalination*, **2013**, **328**:42-50
- [10] Crini G. *Bioresour. Technol.*, **2006**,**97**(9):1061-1085
- [11] Aguado J, Van Grieken R, L pez-Muoz M J, et al. *Appl. Catal. A*, **2006**,**312**:202-212
- [12] Gao B J, Gao Y C, Li Y B. *Chem. Eng. J.*, **2010**,**158**:542-549
- [13] Otsuka R, Yoshitake H. *J. Colloid Interface Sci.*, **2014**,**415**: 143-150
- [14] Chen J, Qu R J, Zhang Y, et al. *Chem. Eng. J.*, **2012**,**209**: 235-244
- [15] Xu L, Liu Y Q, Hu H P, et al. *Desalination*, **2012**,**294**:1-7
- [16] Tian Y, Yin P, Qu R J, et al. *Chem. Eng. J.*, **2010**,**162**(2): 573-579
- [17] Moritz M. *Appl. Surf. Sci.*, **2013**,**283**:537-545
- [18] Ayad M M, El-Nasr A A. *J. Nanostruct. Chem.*, **2013**,**3**:3-11
- [19] Santos D O, Santos M L N, Costa J A S, et al. *Environ. Sci. Pollut. Res.*, **2013**,**20**(12):5028-5035
- [20] Monash P, Pugazhenth G. *Adsorption*, **2009**,**15**:390-405
- [21] Baruah A, Kumar S, Vaidya S, et al. *J. Fluorescence*, **2013**, **23**(5):1287-1292
- [22] Pitoniak E, Wu C Y, Londeree D, et al. *J. Nanopart. Res.*, **2003**,**5**(3/4):281-292
- [23] Neghlani P K, Rafizadeh M, Taromi F A. *J. Hazard Mater.*, **2011**,**186**(1):182-189
- [24] Jung K Y, Park S B. *Appl. Catal. B*, **2000**,**25**:249-256
- [25] Xu R, Jia M, Li F T, et al. *Appl. Phys. A*, **2012**,**106**(3):747-755
- [26] Xaviera R J, Gobinath E. *Spectrochim. Acta A*, **2012**,**86**: 242-251
- [27] Xue X M, Li F T. *Microporous Mesoporous Mater.*, **2008**, **116**:116-122
- [28] Gupta V K, Mohan D, Sharma S, et al. *Sep. Sci. Technol.*, **2000**,**35**(13):2097-2113
- [29] Li L, Liu S X, Zhu T. *J. Environ. Sci.*, **2010**,**22**(8):1273-1280
- [30] Zeng X W, Fan Y G, Wu G L, et al. *J. Hazard Mater.*, **2009**, **169**(1/2/3):1022-1028
- [31] Bayramo lu G, Bektas S, Arica M Y. *J. Hazard Mater.*, **2003**, **101**:285-300
- [32] Chegrouche S, Mellah A, Telmoune S. *Water Res.*, **1997**,**31**: 1733-1737
- [33] Yu Q, Deng S B, Yu G. *Water Res.*, **2008**,**42**:3089-3097
- [34] Zhang Z Y, Zhang Z B, Fern ndez Y. et al. *Appl. Surf. Sci.*, **2010**,**256**(8):2569-2576
- [35] Wang Q, Chen C C, Zhao D, et al. *Langmuir*, **2008**,**24**:7338-7345